Förster resonance energy transfer photoacoustic microscopy

Yu Wang, Lihong V. Wang

Yu Wang, Lihong V. Wang, "Förster resonance energy transfer photoacoustic microscopy," Proc. SPIE 8581, Photons Plus Ultrasound: Imaging and Sensing 2013, 85812E (4 March 2013); doi: 10.1117/12.2004150

SPIE.

Event: SPIE BiOS, 2013, San Francisco, California, United States

Förster resonance energy transfer photoacoustic microscopy

Yu Wang and Lihong V. Wang*

Optical Imaging Laboratory, Dept. of Biomedical Engineering, Washington University in St. Louis, 1 Brookings Dr., St. Louis, MO, USA 63130

ABSTRACT

Förster resonance energy transfer (FRET) provides fluorescence signals sensitive to intra- and inter-molecular distances in the 1-10 nm range. Widely applied in the optical imaging environment, FRET enables visualization of physicochemical processes in molecular interactions and conformation changes. We reported photoacoustic imaging of FRET, based on non-radiative decay that produces heat and subsequent acoustic waves. The experimental results show that photoacoustic imaging offers better penetration into scattering biological tissue. Through its ability to three-dimensionally image tissue with scalable resolution, photoacoustic microscopy provides a beneficial biomedical tool to broaden the in vivo application of the FRET technique.

Keywords: Förster resonance energy transfer, FRET, Photoacoustic imaging,

1. INTRODUCTION

Förster, or fluorescence, resonance energy transfer (FRET) is a physical process in which energy is transferred from an excited donor fluorophore to adjacent chromophores non-radiatively [1, 2]. Because the transfer rate is sensitive to the donor-acceptor distance, FRET provides a molecular ruler for measuring distances between biomolecules. FRET has proven to be a tool of immense value to understand biological processes such as protein interactions and conformational changes, and in vivo applications have been explored for the study of protease activity, protein misfolding, and intracellular calcium.

Photoacoustic (PA) microscopy is an emerging biomedical imaging modality based on detecting non-radiative decay [3-8]. In the absence of photochemical decay, non-radiative decay converts the excited molecular state energy into heat. With pulsed light excitation, the heat induces thermoelastic expansion, generating acoustic waves in the medium. An ultrasonic transducer is used to detect the acoustic energy, which enables PA imaging of non-radiative decay processes.

The occurrence of FRET manifests itself through the reduction of donor fluorescence emission because of the non-radiative energy transfer to the acceptor, increasing both the fluorescence and PA emissions from the acceptor. The conversion efficiency of the transferred energy to photoacoustic emission depends on the quantum yield of the acceptor. In the case of a non-fluorescent acceptor, an increase of the PA signal strength becomes the solitary yield of the donor fluorescence quenching.

Compared with the fluorescence technique, PA imaging of FRET has inherent merits. By utilizing low ultrasonic scattering, PA imaging enables high-resolution, deeply penetrating imaging in biological tissue. Moreover, PA imaging is scalable with optical illumination and ultrasonic detection parameters. It can be designed to provide either sub-micron resolution at a shallow depth or a centimeter penetration depth while a high depth to resolution ratio is maintained. Therefore, the ultimate applications of FRET extending from live cells to organs in vivo can potentially benefit from the multi-scale PA imaging capability.

* lhwang@seas.wustl.edu; labs.seas.wustl.edu/bme/Wang/

Photons Plus Ultrasound: Imaging and Sensing 2013, edited by Alexander A. Oraevsky, Lihong V. Wang,
Proc. of SPIE Vol. 8581, 85812E · © 2013 SPIE · CCC code: 1605-7422/13/$18 · doi: 10.1117/12.2004150

2. METHODS

FRET involves the non-radiative transfer of excited state energy from a fluorophore (the donor D) to another nearby absorbing (but not necessarily fluorescent) molecule (the acceptor A) [9]. The energy transfer efficiency E, which directly measures the fraction of photon energy absorbed by the donor that is transferred to the nearby acceptor, can be expressed as follows.

$$E = \frac{k_t}{k_f + k_t + k_{nr}} = [1 + (r / R_0)^6]^{-1} \tag{1}$$

where k_f , k_t , and k_{nr} are the donor fluorescence emission rate, the FRET rate from the donor to the acceptor, and other non-radiative decay rate of the donor, respectively; *r* is the intra- or inter-molecular distance; R_0 is the critical transfer distance characteristic of a given donor-acceptor pair, in the range of 1-10 nm. The distance *r* is an important parameter for describing biomolecules engaged in complex formation and conformational transition.

In our experiment, a pair consisting of a donor fluorophore (Rhodamine 6G) and a non-fluorescent acceptor chromophore (DQOCI) was examined. The energy transferred from the donor to the non-fluorescent acceptor increases the PA signal.

Förster's theory predicts that, due to decreasing r, the energy transfer efficiency E increases with increasing acceptor concentration C . For an ensemble of donor and acceptor molecules, the FRET efficiency E is summed over the energy transfer channels to all acceptor molecules around the excited donor molecule, and is given by,

$$E = \sqrt{\pi} x \exp(x^2)\{1 - \mathrm{erf}(x)\} \tag{2}$$

where $\mathrm{erf}(x)$ is the error function, and $x = \frac{C}{C_0}$. The critical concentration C_0 is defined by $C_0 = \frac{3}{4\pi N_A R_0^3}$, where N_A is Avogadro's number; C_0 corresponds to an average of one acceptor molecule in a sphere of radius R_0. In our experiment, the concentrations of the acceptor varied between ~10^{-4} and ~10^{-3} molar, while the concentration of the donor was held constant as typically practiced in FRET solution studies.

The fluorescence quantum yields of donor Rhodamine 6G in the absence and presence of acceptor DQOCI, Q_D and Q_{DA}, are determined by the ratio of the fluorescence emission rate to the total decay rate.

$$Q_D = \frac{k_f}{k_f + k_{nr}} \tag{3}$$

$$Q_{DA} = \frac{k_f}{k_f + k_{nr} + k_t} \tag{4}$$

The subscripts *D* and *A* denote the presence of the donor and the acceptor, respectively. Therefore, the energy transfer efficiency E can be measured as

$$E = 1 - \frac{Q_{DA}}{Q_D} \tag{5}$$

The fluorescence intensities F from the donor in the absence and presence of acceptor DQOCI are given by

$$F_D \propto \mu_{a,D}(\lambda_{ex}) Q_D \frac{\lambda_{ex}}{\lambda_f} \tag{6}$$

$$F_{DA} \propto \mu_{a,D}(\lambda_{ex}) Q_{DA} \frac{\lambda_{ex}}{\lambda_f} \tag{7}$$

where $\mu_{a,D}$ is the absorption coefficient of the donor at the excitation wavelength. The ratio of the excitation wavelength λ_{ex} to the fluorescence emission wavelength λ_f accounts for the Stokes shift of fluorescence emission.

The PA amplitudes P can be calculated as

$$P_D \propto \mu_{a,D}(\lambda_{ex})(1 - Q_D \frac{\lambda_{ex}}{\lambda_f}) \tag{8}$$

$$P_{DA} \propto \mu_{a,D}(\lambda_{ex})(1 - Q_{DA} \frac{\lambda_{ex}}{\lambda_f}) \tag{9}$$

Note that P_{DA} is attributed to both the k_t and donor's k_{nr} decay pathways, i.e., the FRET decay through the acceptor pathway in addition to the non-radiative decay through the donor pathway.

In fluorescence microscopy, the energy transfer efficiency *E* can be computed by

$$E = 1 - \frac{F_{DA}}{F_D} \tag{10}$$

Similarly, the ratio of the PA amplitudes yields

$$\frac{P_{DA}}{P_D} = \frac{1 - Q_{DA} \frac{\lambda_{ex}}{\lambda_f}}{1 - Q_D \frac{\lambda_{ex}}{\lambda_f}} \tag{11}$$

From Eq. (11), the donor quantum yield in the presence of the acceptor Q_{DA} can be calculated as

$$Q_{DA} = [1 - \frac{P_{DA}}{P_D}(1 - Q_D \frac{\lambda_{ex}}{\lambda_f})] \frac{\lambda_f}{\lambda_{ex}} \tag{12}$$

From Eqs. (5) and (12), one can compute the transfer efficiency as follows if the characteristic parameter $Q_D \frac{\lambda_{ex}}{\lambda_f}$ of the donor is known:

$$
\begin{aligned}
E &= 1 - \frac{Q_{DA}}{Q_D} \\
&= 1 - [1 - \frac{P_{DA}}{P_D}(1 - Q_D \frac{\lambda_{ex}}{\lambda_f})] \frac{\lambda_f}{\lambda_{ex} Q_D} \\
&= 1 - [\frac{\lambda_f}{\lambda_{ex}} - \frac{P_{DA}}{P_D}(\frac{\lambda_f}{\lambda_{ex}} - Q_D)] \frac{1}{Q_D} \\
&= \frac{Q_D - [\frac{\lambda_f}{\lambda_{ex}} - \frac{P_{DA}}{P_D}(\frac{\lambda_f}{\lambda_{ex}} - Q_D)]}{Q_D} \\
&= \frac{Q_D - \frac{\lambda_f}{\lambda_{ex}} + \frac{P_{DA}}{P_D}\frac{\lambda_f}{\lambda_{ex}} - \frac{P_{DA}}{P_D} Q_D}{Q_D} \\
&= \frac{Q_D(1 - \frac{P_{DA}}{P_D}) - \frac{\lambda_f}{\lambda_{ex}}(1 - \frac{P_{DA}}{P_D})}{Q_D} \\
&= \frac{(1 - \frac{P_{DA}}{P_D})(Q_D - \frac{\lambda_f}{\lambda_{ex}})}{Q_D} \\
&= (\frac{P_{DA}}{P_D} - 1)(\frac{\lambda_f}{\lambda_{ex} Q_D} - 1)
\end{aligned}
\tag{13}
$$

The strong spectral overlap of the donor and acceptor required for FRET imaging leads to the acceptor bleed-through (ABT) contamination, i.e., the direct excitation of acceptor at the donor's excitation wavelength. For quantitative treatment of FRET, we remove the ABT background P_{ABT} from the raw PA signal. The corrected PA signal P_{DA} at λ_{ex} is obtained as follows:

$$
P_{DA}(\lambda_{ex}) = P_{DA}^{raw}(\lambda_{ex}) - P_{ABT}(\lambda_{ex}) \tag{14}
$$

where $P_{DA}^{raw}(\lambda_{ex})$ is the raw PA amplitude measured from the FRET dye system at λ_{ex}.

3. RESULTS

PA and fluorescence images were acquired using the integrated dual-modality PA and fluorescence confocal microscope (Fig. 1) [10, 11]. Based on solutions containing a controlled amount of donor Rhodamine 6G and acceptor DQOCI, the PA and fluorescence imaging of FRET efficiency is analyzed. Seven stock ethanol solutions were prepared with different concentrations of donor Rhodamine 6G and acceptor DQOCI as tabulated in Fig. 2.

The sample solutions were injected into 7 glass tubes (VWR; inner diameter: 0.56 mm; outer diameter: 0.8 mm) and sealed using epoxy to avoid evaporation of ethanol.

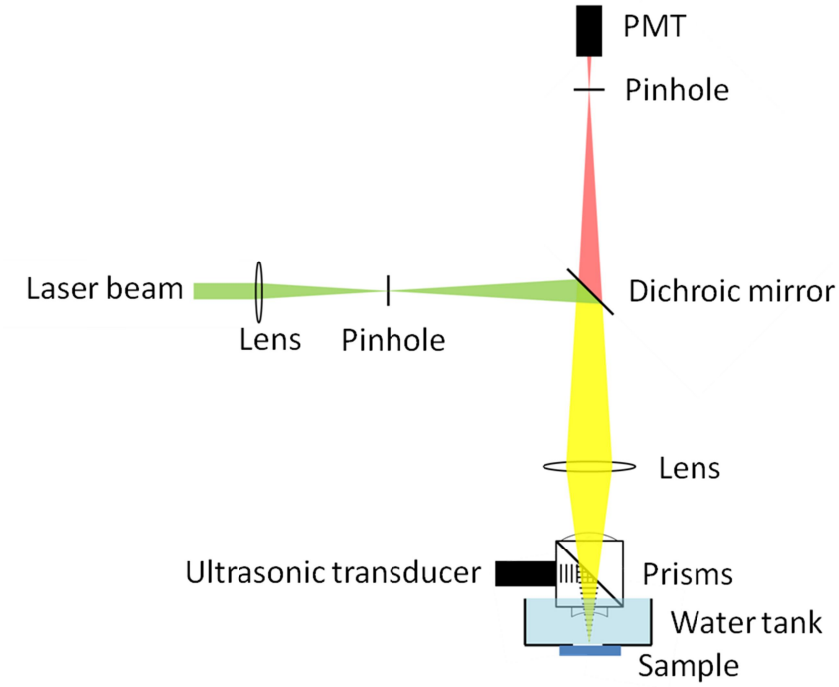

Figure 1. Schematic of the dual-modality fluorescence and photoacoustic microscope.

Donor: R6G [10^{-4} M]	5	0	5	0	5	0	5
Acceptor: DQOCI [10^{-4} M]	0	1.25	1.25	2.5	2.5	5	5

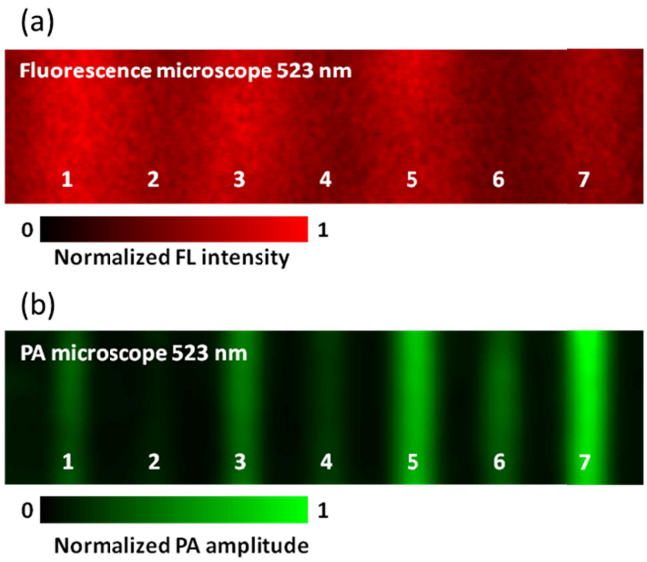

Figure 2. (a) Fluorescence microscopic image acquired at 523 nm of the tube phantom. (b) *En-face* photoacoustic microscopic image acquired at 523 nm.

To test the feasibility of imaging in biological tissue, freshly excised 1 mm thickness rat skin tissue was overlaid on the tubes. While the donor Rhodamine 6G is excited, fluorescence and photoacoustic emission is detected in the presence of different concentrations of acceptor DQOCI. Compared with a solution containing only donor Rhodamine 6G (tube No. 1), the mixtures containing both donor Rhodamine 6G and acceptor DQOCI have diminished fluorescence signals (tube No. 3, 5 and 7). More acceptor DQOCI made fluorescence quenching more effective. The detected tubes in the fluorescence confocal image were severely blurred due to light scattering in the tissue (Fig. 2(a)). The *en-face* PA MAP image (Figs. 2(b)) clearly shows FRET quenching of the donor Rhodamine 6G fluorescence by acceptor DQOCI. Figure 3 shows the FRET efficiency map of the tissue phantom calculated from the PA image, whereas a similar map cannot be generated from Fig. 2(a) due to its poor signal-to-noise ratio. The results demonstrate the potential for in vivo FRET imaging using the PA method.

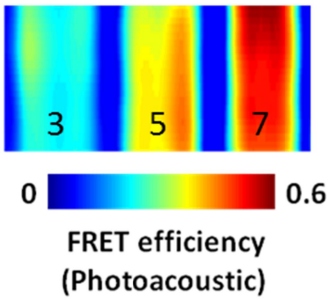

Figure 3. FRET efficiency map acquired using the photoacoustic microscope.

In conclusion, PA microscopy has been used to image FRET efficiencies through a 1-mm-thick skin tissue. Based on the relative increase of PA signals, absolute FRET efficiency can be quantified. Compared with confocal microscopy, PA microscopy offers better penetration into scattering biological tissue [12]. Future work will extend PA FRET imaging to in vivo animal studies.

REFERENCES

[1] T. Forster, "Energy migration and fluorescence," Journal of Biomedical Optics **17**, 011002 (2012).
[2] E. A. Jares-Erijman, and T. M. Jovin, "FRET imaging," Nature Biotechnology **21**, 1387-1395 (2003).
[3] Y. Wang, K. Maslov, and L. H. V. Wang, "Spectrally encoded photoacoustic microscopy using a digital mirror device," Journal of Biomedical Optics **17**, 066020 (2012).
[4] Y. Wang, T. N. Erpelding, L. Jankovic, Z. J. Guo, J. L. Robert, G. David, and L. H. V. Wang, "In vivo three-dimensional photoacoustic imaging based on a clinical matrix array ultrasound probe," Journal of Biomedical Optics **17**, 061208 (2012).
[5] Y. Wang, K. Maslov, Y. Zhang, S. Hu, L. M. Yang, Y. N. Xia, J. A. Liu, and L. H. V. Wang, "Fiber-laser-based photoacoustic microscopy and melanoma cell detection," Journal of Biomedical Optics **16**, 011014 (2011).
[6] D. Razansky, C. Vinegoni, and V. Ntziachristos, "Multispectral photoacoustic imaging of fluorochromes in small animals," Optics Letters **32**, 2891-2893 (2007).
[7] L. H. V. Wang, and S. Hu, "Photoacoustic Tomography: In Vivo Imaging from Organelles to Organs," Science **335**, 1458-1462 (2012).
[8] H. P. Brecht, R. Su, M. Fronheiser, S. A. Ermilov, A. Conjusteau, and A. A. Oraevsky, "Whole-body three-dimensional optoacoustic tomography system for small animals," J Biomed Opt **14**, 064007 (2009).
[9] C. Berney, and G. Danuser, "FRET or no FRET: A quantitative comparison," Biophysical Journal **84**, 3992-4010 (2003).

[10] Y. Wang, S. Hu, K. Maslov, Y. Zhang, Y. N. Xia, and L. V. Wang, "In vivo integrated photoacoustic and confocal microscopy of hemoglobin oxygen saturation and oxygen partial pressure," Optics Letters **36**, 1029-1031 (2011).
[11] Y. Wang, K. Maslov, C. Kim, S. Hu, and L. H. V. Wang, "Integrated Photoacoustic and Fluorescence Confocal Microscopy," IEEE Transactions on Biomedical Engineering **57**, 2576-2578 (2010).
[12] Y. Wang, and L. V. Wang, "Forster resonance energy transfer photoacoustic microscopy," Journal of Biomedical Optics **17**, 086007 (2012).